Chitosan cross-linked poly(acrylic acid) hydrogels: drug release control and mechanism

Wang, Yiming; Wang, Jie; Yuan, Zhenyu; Han, Haoya; Li, Tao; Li, Li; Guo, Xuhong

DOI
10.1016/j.colsurfb.2017.01.008

Publication date
2017

Document Version
Accepted author manuscript

Published in
Colloids and Surfaces B: Biointerfaces

Chitosan Cross-linked Poly(acrylic acid) Hydrogels: Drug Release Control and Mechanism

Yiming Wang[a,b], Jie Wang*[,a], Zhenyu Yuan[a], Haoya Han[a,c], Tao Li[a], Li Li[a], and Xuhong Guo*[,a,d]

[a] State Key Laboratory of Chemical Engineering, East China University of Science and Technology, Meilong Road 130, 200237 Shanghai, China

[b] Advanced Soft Matter Group, Department of Chemical Engineering, Delft University of Technology, van der Maasweg, 2629 HZ Delft, The Netherlands

[c] Stranski-Laboratorium für Physikalische und Theoretische Chemie, Technische Universität Berlin, Strasse des 17. Juni 124, D-10623 Berlin, Germany

[d] Engineering Research Center of Materials Chemical Engineering of Xinjiang Bingtuan , Shihezi University, Xinjiang 832000, China

*To whom correspondence should be addressed. Tel: +86 021 64253789, Fax: +86 021 64253159. E-mail: jiewang2010@ecust.edu.cn (Jie Wang), or guoxuhong@ecust.edu.cn (Xuhong Guo).

Abstract: Chitosan has been used to cross-link poly(acrylic acid) to give three pH-sensitive hydrogels designed to control the release of the drugs amoxicillin and meloxicam. The extent of cross-linking and solution pH was found to dominate the swelling behavior of these hydrogels as shown by scanning electron microscopy and swelling time dependencies. The rates of release of amoxicillin and meloxicam from the loaded hydrogels increased with increase in pH consistent with the extent of hydrogen bonding between hydrogel components and between the hydrogel and the drugs being important determinants of release rate. Both the Korsemeyer-Peppas and Weibull models fitted release data consistent with drug release occurred through a combination of drug diffusion and hydrogel relaxation processes. These hydrogels appear to provide an ideal basis for controlled drug delivery systems.

Keywords: Chitosan, pH sensitive hydrogel, Drug delivery, Release mechanism

1. Introduction

Hydrogels are generally composed of hydrophilic organic networks which incorporate large amounts of water into their structures. This renders them both soft and elastic properties which are compatible with human physiology. Many hydrogels are also able to load a wide variety of drugs into their structures and substantially protect them from physiological conditions, particularly those of the stomach were pH is low and enzyme concentrations are high; conditions under which many drugs are

unstable. In addition to this protective characteristic, hydrogels may potentially be designed to selectively release drugs under the physiological conditions at the disease site in the body, and thereby achieve a targeted drug release. Consequently, hydrogels have found wide application in drug delivery studies [1-4]. In addition to these characteristics, the introduction of stimuli dependent phase changes into hydrogels offers the possibility of developing sophisticated controlled drug release systems. Examples of such stimuli are light [5], temperature [6] and pH change [7].

Apart from being physically compatible with human physiology, hydrogels must also be biocompatible with body chemistry if they are to be viable as drug delivery systems. Fortunately, there is range of biocompatible polymers which may be converted to hydrogel networks through chemically cross-linking them. However, it must be ensured that such cross-linking entities are not toxic [8-10]. While cross-linking through physical interactions such as hydrogen bonding or hydrophobic interactions has been proposed to avoid toxicity problems [11-13], such cross-linking may be not be strong enough to produce a sufficiently stable hydrogel for effective drug loading. Fortunately, polysaccharides may be used as chemical cross-linkers to produce biocompatible hydrogels which present attractive applications in drug delivery [14-17].

The naturally occurring polysaccharide chitosan (CS) has been shown to be amenable to functionalization to produce a range of versatile materials with substantial potential for biomedical applications [18-22]. In this work, a chitosan derivative is used to cross-link poly(acrylic acid) (PAA) to give three pH sensitive

poly(acrylic acid)/chitosan hydrogels (PAACS-I, PAACS-II and PAACS-III) in which the extent of chitosan cross-linking progressively increases, and which are designed to control the release of the drugs amoxicillin and meloxicam (Scheme 1). These drug releases are analyzed through the Korsemeyer-Peppas and Weibull drug release models [23,24] to gain insight into the drug release mechanism and thereby improved understanding for the design of more advanced and reliable hydrogel drug delivery systems.

Scheme 1. Molecular structures of amoxicillin and meloxicam.

2. Experimental

2.1 Materials:

Chitosan (CS, degree of *N*-deacetylation = 95%, Mw = 200 kDa) was purchased from Aoxing Biotechnology Co. Ltd., China. Maleic anhydride (MAH, 99%) was purchased from Acros Co. Ltd. Ammonium persulfate (APS, 99%) and acrylic acid (AA, 99%, distilled under vacuum pressure prior to use) were provided by Sigma Aldrich. Amoxicillin and meloxicam were supplied by TCI, Japan. The water used in all experiments was purified by reverse osmosis (Shanghai RO Micro Q). All other reagents and solvents were used directly.

2.2 Synthesis of chitosan-g-(maleic anhydride) (CSMAH)

An aqueous solution of chitosan was prepared by dissolving 0.5 g of chitosan in

40 mL of 2.5 wt% acetic acid aqueous solution under vigorous stirring. Subsequently, 2.5 g maleic anhydride in 1 mL acetone were added slowly into the pre-prepared chitosan solution under ice cooling within 10 min. The reaction mixture was allowed to warm to room temperature and stand for 8 h. Finally, the viscous solution was poured into 500 mL of acetone to precipitate the product. The solid product was purified by extraction with acetone three times and subsequent drying under vacuum at 50 ^{o}C for 48 h.

2.3 Preparation of PAACS hydrogels

The three hydrogels, PAACS-I, PAACS-II and PAACS-III, were prepared through free radical polymerization, using APS as an initiator and the synthesized CSMAH as a cross-linker. Briefly, to a solution of 1.4 g NaOH in 40 mL water at room temperature, either 0.05, 0.10 or 0.15 g of CSMAH were added (for PAACS-I, PAACS-II and PAACS-III, respectively) with stirring until a transparent solution was obtained, whereupon 0.01 g APS was added (Table 1). These mixtures were each transferred into a reaction vessel and a N_2 stream was passed through for 30 min to eliminate dissolved oxygen. The copolymerizations were carried out at 70 ^{o}C for 2 h. The gained hydrogels were placed in 500 mL of methanol/water (v/v = 7/3) for 24 h to remove the residual reactants. Finally, the purified hydrogels were cut into thin cylindersand dried to constant weight in an oven at 60 ^{o}C (hydrogel samples with 60 mg in weight, 2.5 mm in diameter, and 20 mm in length).

Table 1. Reactants amounts for the preparation of PAACS hydrogels.

Hydrogel	AA (g)	CSMAH (g)	APS (g)	NaOH (g)	Deionized Water (mL)
PAACS-I	2.8	0.05	0.01	1.4	40
PAACS-II	2.8	0.10	0.01	1.4	40
PAACS-III	2.8	0.15	0.01	1.4	40

2.4 Determination of the hydrogel swelling ratios (*SR*)

The dried hydrogel (0.5 g) was immersed in the 100 mL of aqueous phosphate buffer solutions at pH 1.2, 6.8, and 7.4. The hydrogels were taken out of solution and weighed after removing the residual solutions on the surface at a pre-determined time interval. The hydrogels were then returned to solution and the process was repeated until a constant *SR* was obtained as calculated through Equation (1), in which m_s and m_d are the weight of the hydrogel in the swollen and dry states, respectively.

$$SR = \frac{m_s - m_d}{m_d} \quad (1)$$

2.5 Rheological measurements

The dynamic frequency sweep measurements were performed on a MCR501 rheometer (Anton-Paar Physical Company). A parallel-plate made of stainless steel with a diameter of 25 mm was used. During all rheological measurements, the upper plate was set at a distance of 1 mm from the down plate. All the hydrogel samples were cut into a cylindrical shape with a thickness of 1 mm and a diameter of 25 mm for the measurement. The elastic modulus (G') and viscous modulus (G'') over a frequency range of 0.1 to 10 Hz were recorded at a constant strain of 1%, which was

in the linear range of the viscoelasticity. All measurements were performed at 37 ^{o}C.

2.6 Drug loading

Amoxicillin and meloxicam were loaded into the PAACS hydrogels by soaking and swelling the dried hydrogels in solutions of drugs according to a reported method [25]. This is exemplified by the loading of amoxicillin for which 60 mg of the dry cylindrical hydrogels were immersed into 50 mL of 200 μg mL^{-1} amoxicillin solutions under moderate stirring for 24 h at 37 ^{o}C. Thereafter, the drug-loaded hydrogels were taken out and rinsed with deionized water to remove any residual drugs from the surface. It should be noticed that meloxicam is poorly water soluble and accordingly a small amount of methanol was added to improve solubility; otherwise the procedure was as for that of amoxicillin. The loaded drug amounts were determined by UV-vis spectroscopy (SHIMADZU UV-2550 UV−vis) based on the decrease of the concentration of drug loading solutions determined from UV-vis calibration curves for amoxicillin and meloxicam at 228 nm and 361 nm, respectively. The encapsulation efficiency (*EE*) and loading content (*LC*) of the drugs were calculated through Equations (2) and (3) where m_e is the amount of encapsulated drug, m_o is the total amount of added drug, and m_d is the amount of the dried hydrogel. The *EE* and *LC* determined are listed in Table S1.

$$EE(\%) = \frac{m_e}{m_o} \times 100 \quad (2)$$

$$LC(\%) = \frac{m_e}{m_d} \times 100 \quad (3)$$

2.7 drug release study

The release of amoxicillin and meloxicam from PAACS hydrogels was carried out in aqueous phosphate buffer solutions at pH 1.2, 6.8, and 7.4 at 37 ^{o}C. Basically, either amoxicillin or meloxicam loaded hydrogel was placed into 60 mL of moderately stirred aqueous buffer solution. At appropriate time intervals, 2.0 mL samples of the aqueous buffer solutions were withdrawn and replaced by 2.0 mL fresh aqueous buffer solutions. The amount of the released drugs in the withdrawn sample was determined by UV-Vis absorbance at 228 nm for amoxicillin and 361 nm for meloxicam according to the molar absorbance calibration curves of amoxicillin and meloxicam. All release data were performed in in triplicate and averaged.

2.8 Characterization

All infrared spectra were obtained from dried samples in KBr pellets using a Nicolet 6700 FTIR spectrophotometer. ^{1}H NMR spectra was taken by a 500 MHz Bruker DRX500 spectrometer at 25 ^{o}C using D_2O as the solvent. The SEM was performed using a Nova Nano SEM 50 field emission scanning electron microscope (FE-SEM) at an acceleration voltage of 3 kV.

3. Results and discussion

As shown in scheme 2, CSMAH was synthesized by grafting MAH onto the main chain of CS. Subsequently, CSMAH was employed to copolymerize with AA to create the three hydrogels in which the extent of CS cross-linking increase in the sequence

PAACS-I < PAACS-II < PAACS-III as a consequence of the three-fold increase in CSMAH concentration used in their respective preparations (Table 1).

(Scheme 2 here)

Structure characterization

Fig. 1A shows the ^{1}H NMR spectrum of CSMAH. The broad peaks at 3.2-4.2 ppm arise from the hydrogens of the pyranose units of CS (H3, H4, H5, and H6), the peak at 3.05 ppm arises from H2, and the peak of methyl hydrogen of the *N*-acetyl groups is located at 2.12 ppm. The two peaks at 5.85 and 6.32 ppm which are referred to H7 and H8 of the grafted MAH. Thus, the ^{1}H NMR characterization indicates that MAH modified CS was successfully synthesized. The averaging grafting degree (GD) of MAH onto CS in CSMAH, defined as the number of grafted MAH per 100 pyranose units, was determined to be 27.3 $\pm$ 0.1 % based on the proton integration (Eq. 4), where $I_{6.32ppm}$ and $I_{3.2\text{-}4.2ppm}$ are the integrated peak area ratios of protons of the MAH and CS components, respectively. It is anticipated that that *GD* varies over a small range between individual chains.

$$GD = \frac{5 \times I_{6.32\,ppm}}{I_{3.2-4.2\,ppm}} \times 100\% \quad (4)$$

FTIR spectra of PAA, CS, CSMAH, and PAACS hydrogels are displayed in Fig. 1B. For PAA , a broad absorption band from 3000 to 3600 cm^{-1} is stemmed from the O-H stretching vibration. The peaks appeared at 1637 and 1151 cm^{-1} are contributed by the stretching vibration of C=O and C-O of the carboxylic group. Another two

peaks appeared at 1454 and 1409 cm^{-1} are caused by the O-H bending vibration of PAA. The characteristic peaks of CS located at 3346 cm^{-1} (O-H and N-H stretching), 2921 and 2854 cm^{-1} (C-H stretching), and 1654 cm^{-1} (NH-CO (I) stretching) can be observed clearly in the FT-IR spectrum. In the CSMAH spectrum, the new peaks appeared at 1658 and 1564 cm^{-1} are attributed to C-O groups of the opened MAH, it further approves the successful modification of CS. The peak at 1700 cm^{-1} is caused by the carboxyl stretching vibration of carboxylic acid. With regard to the spectrum of PAACS hydrogel, some absorption peaks are changed by comparing with CSMAH and PAA. A broad peak at the range of 3000-3500 cm^{-1} arises from the overlapping of the O-H stretching vibrations of PAA and N-H stretching vibrations of CSMAH. The characteristic stretching absorption band of C=O in PAA presents at 1637 cm^{-1}. In particular, the characteristic absorption bands of CS at 2921 and 2854 cm^{-1} consistent with the participation of CSMAH in the polymerization to for PAACS hydrogels.

(Fig. 1 here)

X-Ray powder diffraction (XRD)

XRD was employed to reveal the crystallinity of CS, CSMAH, PAA, PAACS-I, PAACS-II and PAACS-III. As shown in Fig. 1C, the XRD pattern of CS shows two major peaks at 10^{o} and 19^{o} which transforms into a single broad peak at 20^{o} in the XRD pattern of CSMAH caused by the grafting of MAH onto CS. Upon polymerization with AA, a substantial decrease in intensity occurs in the region

centered at 10^o where both CS and CSMAH absorb, and the broad peaks of PAA appear in the range 15^o-40^o. This is consistent with the copolymerization of CSMAH and AA progressing in a random way and a consequent decrease in crystallinity by comparison with that of CS, and also a decrease in inter- and intra-molecular hydrogen bonding.

Rheology

The rheological properties are important indicators of soft materials performances [26]. As shown in Fig. 1D, for each of the three hydrogels, PAACS-I, PAACS-II and PAACS-III, the elastic modulus, *G'*, was higher than their viscous modulus, *G"*, over the measured frequency range. This is consistent with the hydrogels being present as solids under the measuring conditions; thereby constituting a stable structure for drug loading. It is also observed that *G*' increases in the sequence PAACS-I < PAACS-II < PAACS-III coincident with the increasing CS cross-linker content. Additionally, the reacted ratio of MAH groups in CSMAH was estimated by Eq. 5, where ρ is the density of PAA, R is the ideal gas constant, T is temperature, and $\bar{M}_c$ is the average molecular weight of PAA between two adjacent cross-linking points [27], here we hypothesize a complete copolymerization is achieved.

$$G = \frac{\rho RT}{\bar{M}_c} \tag{5}$$

The calculation results demonstrated that the cross-linking efficiency is not very high which might stem from the big molecular volume of chitosan, for instance, only ~0.5% MAH groups in CSMAH was presented in cross-linking PAA chains (Fig. 1D).

238 This is also responsible for the low elastic modulus of these hydrogels.

239

240 **Morphology of PAACS hydrogels**

241 The micro-morphologies of the freeze-dried PAACS hydrogels were shown to
242 possess well-defined network structures by SEM (Fig. 2). A statistical analyses of the
243 pore size of these hydrogels indicated that increase in the extent of CS cross-linking
244 significantly decreased pore size. The average pore size of PAACS-I is around ~126
245 μm, while those of PAACS-II and PAACS-III are smaller, ~86 and ~51 μm,
246 respectively. While it has been proposed that the pore size of the hydrogel depends on
247 the size of the ice crystals which are formed during the freeze-drying treatment of the
248 samples [28], the greater the extent of CS cross-linking the greater will be the restraint
249 on the capacity of the hydrogel to swell with water absorption. As a result, the size of
250 the ice crystals and hydrogel pores will decrease with increase in CS cross-linking [29,
251 30].

252

253 **(Fig. 2 here)**

254

255 **Swelling behavior**

256 The swelling properties of PAACS hydrogels were investigated by soaking the
257 freeze-dried hydrogels in aqueous buffer solutions at pH 1.2, 6.8 and 7.7 and
258 recording the weight changes with time at 37 ^{o}C. It is seen from Fig. 3 that PAACS-I,
259 PAACS-II and PAACS-III each exhibits an increase in swelling ratio (*SR*) as pH

increases. It is also seen that at a given pH *SR* decreases in the sequence PAACS-I > PAACS-II > PAACS-III as the extent of CS cross-linking increases. At pH 1.2, the carboxylic acid groups in PAA chains are almost protonated and substantial hydrogen-bonding occurs between them and the repulsion force between polymer chains in the networks is reduced so that the water diffusion into the hydrogel is impeded and swelling is reduced [31-34]. However, at pH 7.4, the carboxylic groups were deprotonated and hydrogen-bonding between them is absent while their negative charges cause electrostatic repulsion between the PAA chains [35]. The overall effect is that the hydrogel network has a looser structure at pH 7.4 than that at pH 1.2 which permits an increased diffusion of water into the hydrogel and an increased swelling.

The effect of pH change on hydrogel swelling superimposes on the increase in the extent CS of cross-linking in the sequence: PAACS-I < PAACS-II < PAACS-III and the corresponding decrease in *SR* in the sequence: PAACS-I > PAACS-II > PAACS-III at the three pH conditions studied. Thus, an increase in CS cross-linking tightens the hydrogel network thereby impeding diffusion of water into it and decreasing the *SR*.

(Fig. 3 here)

Study of pH triggered drug release

The release curves for amoxicillin and meloxicam are displayed in Fig. 4. It demonstrated drug release rate decreases in the hydrogel sequence PAACS-I >

PAACS-II > PAACS-III and that for each hydrogel the release rate increases with increase in pH. This pattern bears a striking similarity to that for the hydrogel *SR* shown in Fig. 3 and suggests that the increase in drug mobility is directly related the increase in hydrogel pore size as pH increases [36].

For PAACS-I, ~30%, ~60% and ~80% of amoxillin is released after 800 min at pH 1.2, 6.8 and 7.4, respectively (Fig. 4). The analogous values for meloxicam are ~20%, ~70% and ~90% at pH 1.2, 6.8 and 7.4, respectively. Both drugs are released more slowly from PAACS-II and PAACS-III, and release from both hydrogels shows an increase in rate with increase in pH. It has been suggested that many drugs are released from hydrogels through a diffusion process which is dominated by the swelling behavior of the hydrogel [36]. Thus, the lower release rate of amoxicillin and meloxicam at pH 1.2 is probably largely contributed by the pore size decrease (Fig. S1) due to greater hydrogen bonding between the PAA and CS chains in hydrogel networks (Scheme 1) and a consequent decrease in hydrogel flexibility and an inhibition of both drug and water diffusion. The hyrogel flexibility is further decreased as cross-linking increases with the consequence that drug release is further slowed as seen from Fig. 4.

It has been revealed that the chemical structure of both the drug and the hydrogel determine the nature and extent of interactions between them and that this impinges on the magnitude of drug release rates [37]. From the release curves for amoxicillin and meloxicam (Fig. 4), we can see obviously that the release rate of amoxicillin is higher than that of meloxicam at pH 1.2 whereas the reverse is the case at pH 6.8 and

7.4. This reflects the variation of the effects of hydrogen bonding between the hydrogel PAA and CS chains and probably between them and the two drugs. Amoxicillin is more hydrophilc than is meloxicam as assessed on the basis of the higher water solubility of amoxicillin. This is likely to diffentiate the behaviour of the two drugs within the hydrogel but a more detailed analysis is not possible on the basis of the currently available data.

(Fig. 4 here)

Mechanism of drug release from hydrogels

The mechanism of drug released from hydrogels may be envisaged as occurring in three main steps as shown in Fig. 5. In the initial step, a), the drug-loaded hydrogel contains a minimum amount of water, the hydrogel exhibits it minimum flexibility, pore size is small and drug mobility is limited. In the second step, b), water diffuses into the hydrogel which undergoes relaxation to become more flexible, pore size grows and drug mobility increases with increased hydration. In the final stage, c), the hydrogel is fully relaxed and hydrated and pore size is at a maximum, as is the rate of drug diffusion from the hydrogel [38, 39].

(Fig. 5 here)

The mathematical modeling of drug release from hydrogel is a facile and an

important approach to understand the elusive release mechanism [24, 39-44]. Accordingly, We have employed both Korsemeyer-Peppas [39-42] and Weibull [24] models to elucidate the release mechanism of amoxicillin and meloxicam. The widely used Korsemeyer-Peppas model expresses the rate of drug release up to the stage where 60% of the drug is released through Eq. 5 where M_t and M_∞ are the amounts of drug released at time t and when equilibrium is reached, respectively; k is a kinetic constant, and n is an exponent typifying the release mechanism.

$$\frac{M_t}{M_\infty} = kt^n \tag{5}$$

The release data for both amoxicillin and meloxicam is well-fitted by Eq. 5 for up to 60 % of drug release as shown in Fig. S1a and c). These fittings correspond to n values in the range beween 0.51 and 0.85 for amoxicillin and between 0.63 and 0.87 for meloxicam (Table S2) consistent with the drugs being released through so-called anomalous diffusion, in which the effects of drug diffusion and hydrogel relaxation are comparable. [36, 39-42]. It can also be seen clearly that at a given pH value, the n values more closely approach 0.89 at which only the relaxation of hydrogel governs the drug release as the extent of cross-linking increases in the sequence PAACS-I < PAACS-II < PAACS-III in the hydrogels [39-42]. That is because increases in cross-linking decrease the hydrogel flexibility such that the hydrogel relaxation process becomes the controlling factor for drug release. The n values characterizing amoxicillin release are smaller than those for meloxicam release which may indicate that amoxicillin interacts more strongly with the hydrogels and is therefore less dependent upon hydrogel relaxation for release. This can also be seen from the

diffusion coefficients of amoxicillin (D_1) and meloxicam (D_2) in the hydrogels (Fig. S3 and Table S3). At higher pH (pH 6.8 and 7.4), we found that the hydrogels relaxed completely within ~300 min, after which the drugs were released in a stable diffusion process. By estimating the diffusion coefficient, we found that D_1 was smaller than D_2 demonstrating the higher interation between amoxicillin and hydrogel. Consequently, the n values for amoxicillin release more closely approach 0.45 (at which only diffusion controls drug release) than is the case for meloxicam. However, the overall conclusion is that both amoxicillin and meloxicam are released from the hydrogels through a combination of diffusion and hydrogel relaxation under the conditions of this study.

As we mentioned previously, Korsemeyer-Peppas equation is only valid for the first 60% of the release curve. In order to give a more reliable mechanism revealing, another model, Weibull model, which covers the entire drug release process, is described through Eq. 6, where a is a constant, and b is an exponent which reflects the underlying release mechanism. A value of b in the range of 0.35 ~ 0.75 signifies a diffusion dominated drug release process and a b value in the range 0.75 ~ 1.0 indicates a combined diffusion and hydrogel relaxation mechanism [24].

$$\frac{M_t}{M_\infty} = 1 - \exp(-at^b) \tag{6}$$

It can be seen from Fig. S2b and d that Eq. 6 can fit the drug release data very well. From the fitting results (Table S2), we can see that most of the b values fall in the range of 0.75~1.0, indicating a combination release process of diffusion and hydrogel relaxation which is in good consistent with the results derived from

Korsemeyer-Peppas model. Thus, it is concluded that both amoxicillin and meloxicam are released from the hydrogels through a combination of diffusion and hydrogel relaxation as was also deduced from the Korsemeyer-Peppas model.

Conclusions

A series of chitosan cross-linked PAACS hydrogels with different degrees of cross-linking were prepared and found an increase in swelling and pore size as pH was increased and as the extent of cross-linking decreased. The drugs amoxicillin and meloxicam were readily loaded into the hydrogels, and their release rates were found to increase with increase in pH and to decrease with increase in cross-linking. Fitting of two models for drug release to the experimental release data indicated that the rates of drug release are controlled to varying extents by a combination of diffusion and hydrogel relaxation.

Acknowledgement

We gratefully acknowledge NSFC Grants (51403062, 21476143 and 51273063), the China Scholarship Council (CSC), China Postdoctoral Science Foundation (2013M541485), 111 Project Grant (B08021), the Fundamental Research Funds for the Central Universities and the Open Project of Engineering Research Center of Materials-Oriented Chemical Engineering of Xinjiang Bingtuan (2015BTRC001) for support of this work.

References

[1] A. Vashist, A. Vashist, Y.K. Gupta and S. Ahmad, Recent advances in hydrogel based drug delivery systems for the human body, J Mater Chem B, 2 (2014) 147-166.

[2] P. Matricardi, C. Di Meo, T. Coviello, W.E. Hennink and F. Alhaique, Interpenetrating Polymer Networks polysaccharide hydrogels for drug delivery and tissue engineering, Advanced Drug Delivery Reviews, 65 (2013) 1172-1187.

[3] D. Costa, A.J.M. Valente, M.G. Miguel and J. Queiroz, Gel Network Photodisruption: A New Strategy for the Codelivery of Plasmid DNA and Drugs, Langmuir, 27 (2011) 13780-13789.

[4] Y. Qiu and K. Park, Environment-sensitive hydrogels for drug delivery, Advanced Drug Delivery Reviews, 64 (2012) 49-60.

[5] M.B. Charati, I. Lee, K.C. Hribar and J.A. Burdick, Light-Sensitive Polypeptide Hydrogel and Nanorod Composites, Small, 6 (2010) 1608-1611.

[6] Z.Q. Lin, W. Gao, H.X. Hu, K. Ma, B. He, W.B. Dai, X.Q. Wang, J.C. Wang, X. Zhang and Q. Zhang, Novel thermo-sensitive hydrogel system with paclitaxel nanocrystals: High drug-loading, sustained drug release and extended local retention guaranteeing better efficacy and lower toxicity, Journal Of Controlled Release, 174 (2014) 161-170.

[7] J.H. Jeong, J.J. Schmidt, C. Cha and H. Kong, Tuning responsiveness and structural integrity of a pH responsive hydrogel using a poly(ethylene glycol)

414 cross-linker, Soft Matter, 6 (2010) 3930-3938.
415 [8] W.E. Hennink and C.F. van Nostrum, Novel crosslinking methods to design
416 hydrogels, Advanced Drug Delivery Reviews, 64 (2012) 223-236.
417 [9] M.T. Popescu, S. Mourtas, G. Pampalakis, S.G. Antimisiaris and C. Tsitsilianis,
418 pH-Responsive Hydrogel/Liposome Soft Nanocomposites For Tuning Drug
419 Release, Biomacromolecules, 12 (2011) 3023-3030.
420 [10] C.X. Ding, L.L. Zhao, F.Y. Liu, J. Cheng, J.X. Gu, Shan-Dan, C.Y. Liu, X.Z. Qu
421 and Z.Z. Yang, Dually Responsive Injectable Hydrogel Prepared by In Situ
422 Cross-Linking of Glycol Chitosan and Benzaldehyde-Capped PEO-PPO-PEO,
423 Biomacromolecules, 11 (2010) 1043-1051.
424 [11] E.A. Appel, R.A. Forster, M.J. Rowland and O.A. Scherman, The control of
425 cargo release from physically crosslinked hydrogels by crosslink dynamics,
426 Biomaterials, 35 (2014) 9897-9903.
427 [12] P. Ilg, Stimuli-responsive hydrogels cross-linked by magnetic nanoparticles, Soft
428 Matter, 9 (2013) 3465-3468.
429 [13] H.B. Zhang, F. Zhang and J. Wu, Physically crosslinked hydrogels from
430 polysaccharides prepared by freeze-thaw technique, React Funct Polym, 73 (2013)
431 923-928.
432 [14] F. Corrente, H.M. Abu Amara, S. Pacelli, P. Paolicelli and M.A. Casadei, Novel
433 injectable and in situ cross-linkable hydrogels of dextran methacrylate and
434 scleroglucan derivatives: Preparation and characterization, Carbohydrate
435 Polymers, 92 (2013) 1033-1039.

436 [15] D. Das, P. Ghosh, S. Dhara, A.B. Panda and S. Pal, Dextrin and Poly(acrylic
437 acid)-Based Biodegradable, Non-Cytotoxic, Chemically Cross-Linked Hydrogel
438 for Sustained Release of Ornidazole and Ciprofloxacin, Acs Appl Mater Inter, 7
439 (2015) 4791-4803.
440 [16] L. Yang, L. Shi, J. Chen, Y. Pei, F. Zhu and Y. Xia, Preparation and
441 Characterization of pH‐sensitive Hydrogel Film of Chitosan/Poly (acrylic acid)
442 Copolymer, in: Macromolecular Symposia, Vol 225, Wiley Online Library,
443 2005, pp. 95-102.
444 [17] L. Shi, L. Yang, J. Chen, Y. Pei, M. Chen, B. Hui and J. Li, Preparation and
445 characterization of pH-sensitive hydrogel of chitosan/poly (acrylic acid)
446 co-polymer, Journal of Biomaterials Science, Polymer Edition, 15 (2004)
447 465-474.
448 [18] Y.M. Wang, J. Wang, T.S. Wang, Y.S. Xu, L. Shi, Y.T. Wu, L. Li and X.H. Guo,
449 Pod-Like Supramicelles with Multicompartment Hydrophobic Cores Prepared by
450 Self-Assembly of Modified Chitosan, Nano-Micro Letters, 8 (2016) 151-156.
451 [19] A.S. Carreira, F.A.M.M. Goncalves, P.V. Mendonca, M.H. Gil and J.F.J. Coelho,
452 Temperature and pH responsive polymers based on chitosan: Applications and
453 new graft copolymerization strategies based on living radical polymerization,
454 Carbohydrate Polymers, 80 (2010) 618-630.
455 [20] Y.M. Wang, J. Wang, H.Y. Han, J.J. Liu, H.Q. Zhao, M.X. Shen, Y.S. Xu, J. Xu,
456 L. Li and X.H. Guo, Self-assembled micelles of N-phthaloylchitosan-g-poly
457 (N-vinylcaprolactam) for temperature-triggered non-steroidal anti-inflammatory

458 drug delivery, J Mater Sci, 51 (2016) 1591-1599.
459 [21] L.M. Hu, Y. Sun and Y. Wu, Advances in chitosan-based drug delivery vehicles,
460 Nanoscale, 5 (2013) 3103-3111.
461 [22] A. Bernkop-Schnurch and S. Dunnhaupt, Chitosan-based drug delivery systems,
462 Eur J Pharm Biopharm, 81 (2012) 463-469.
463 [23] R.W. Korsmeyer, R. Gurny, E. Doelker, P. Buri and N.A. Peppas, Mechanisms
464 Of Solute Release From Porous Hydrophilic Polymers, Int J Pharmaceut, 15
465 (1983) 25-35.
466 [24] V. Papadopoulou, K. Kosmidis, M. Vlachou and P. Macheras, On the use of the
467 Weibull function for the discernment of drug release mechanisms, Int J
468 Pharmaceut, 309 (2006) 44-50.
469 [25] P. Gupta, K. Vermani and S. Garg, Hydrogels: from controlled release to
470 pH-responsive drug delivery, Drug Discov Today, 7 (2002) 569-579.
471 [26] K.L. Liu, Z.X. Zhang and J. Li, Supramolecular hydrogels based on
472 cyclodextrin-polymer polypseudorotaxanes: materials design and hydrogel
473 properties, Soft Matter, 7 (2011) 11290-11297.
474 [27] M. Oyen, Mechanical characterisation of hydrogel materials, International
475 Materials Reviews, 59 (2014) 44-59.
476 [28] X. Hu, W. Wei, X. Qi, H. Yu, L. Feng, J. Li, S. Wang, J. Zhang and W. Dong,
477 Preparation and characterization of a novel pH-sensitive Salecan-g-poly(acrylic
478 acid) hydrogel for controlled release of doxorubicin, J. Mater. Chem. B, 3 (2015)
479 2685-2697.

480 [29] M. Jaiswal, A.K. Dinda, A. Gupta and V. Koul, Polycaprolactone diacrylate
481 crosslinked biodegradable semi-interpenetrating networks of polyacrylamide and
482 gelatin for controlled drug delivery, Biomedical Materials, 5 (2010) 065014.
483 [30] M.-K. Yoo, H.Y. Kweon, K.-G. Lee, H.-C. Lee and C.-S. Cho, Preparation of
484 semi-interpenetrating polymer networks composed of silk fibroin and poloxamer
485 macromer, International journal of biological macromolecules, 34 (2004)
486 263-270.
487 [31] X. Gao, C. He, C. Xiao, X. Zhuang and X. Chen, Biodegradable pH-responsive
488 polyacrylic acid derivative hydrogels with tunable swelling behavior for oral
489 delivery of insulin, Polymer, 54 (2013) 1786-1793.
490 [32] S. Hua, H. Ma, X. Li, H. Yang and A. Wang, pH-sensitive sodium alginate/poly
491 (vinyl alcohol) hydrogel beads prepared by combined Ca 2+ crosslinking and
492 freeze-thawing cycles for controlled release of diclofenac sodium, International
493 journal of biological macromolecules, 46 (2010) 517-523.
494 [33] A. Shefer, A.J. Grodzinsky, K.L. Prime and J.P. Busnel, Novel model networks
495 of poly (acrylic acid): synthesis and characterization, Macromolecules, 26 (1993)
496 5009-5014.
497 [34] F. Oosawa, Polyelectrolytes, in: Polyelectrolytes, Marcel Dekker, 1971.
498
499 [35] R. Jin, L.M. Teixeira, P.J. Dijkstra, M. Karperien, C. Van Blitterswijk, Z. Zhong
500 and J. Feijen, Injectable chitosan-based hydrogels for cartilage tissue
501 engineering, Biomaterials, 30 (2009) 2544-2551.

[36] D. Das, R. Das, P. Ghosh, S. Dhara, A.B. Panda and S. Pal, Dextrin cross linked with poly(HEMA): a novel hydrogel for colon specific delivery of ornidazole, Rsc Adv, 3 (2013) 25340-25350.

[37] G.R. Bardajee, A. Pourjavadi and R. Soleyman, Novel nano-porous hydrogel as a carrier matrix for oral delivery of tetracycline hydrochloride, Colloid Surface A, 392 (2011) 16-24.

[38] S. Kiortsis, K. Kachrimanis, T. Broussali and S. Malamataris, Drug release from tableted wet granulations comprising cellulosic (HPMC or HPC) and hydrophobic component, Eur J Pharm Biopharm, 59 (2005) 73-83.

[39] N. A. Peppas, Analysis of Fickian and non-Fickian drug release from polymers, Pharm. Acta. Helv., 60 (1985) 110-111.

[40] P. L. Ritger and N. A. Peppas, A simple equation for description of solute release II. Fickian and anomalous release from swellable devices, J. Controll. Release, 5 (1987) 37-42.

[41] N. A. Peppas and J. J. Sahlin, A simple equation for the description of solute release. III. Coupling of diffusion and relaxation. Int. J. Pharm., 57 (1989) 169-172.

[42] J. Siepmann and F. Siepmann, Mathematical modeling of drug delivery, Int J Pharmaceut, 364 (2008) 328-343.

[43] J. Siepmann and N.A. Peppas, Modeling of drug release from delivery systems based on hydroxypropyl methylcellulose (HPMC), Advanced Drug Delivery Reviews, 48 (2001) 139-157.

[44] K. Kosmidis, E. Rinaki, P. Argyrakis and P. Macheras, Analysis of Case II drug transport with radial and axial release from cylinders, Int J Pharmaceut, 254 (2003) 183-188.

Graphical abstract:

Drug loaded chitosan cross-linked poly(acrylate) hydrogels exhibit pH-dependent drug release through a mechanism involving drug diffusion and hydrogel relaxation.

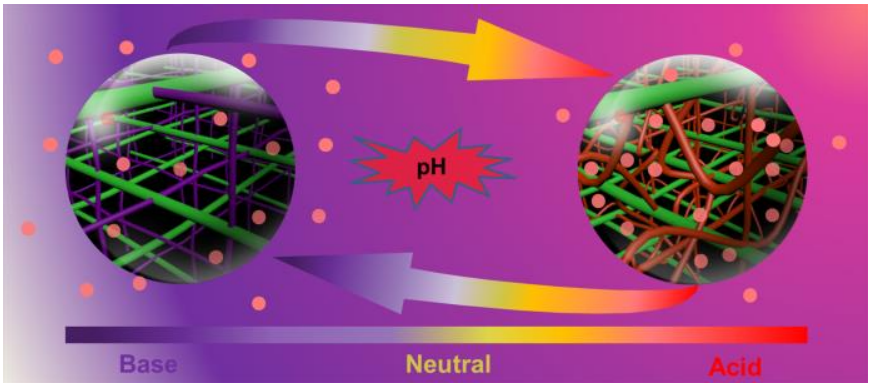

Figure Captions

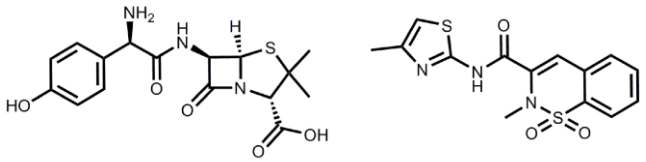

Scheme 1. Molecular structures of amoxicillin and meloxicam.

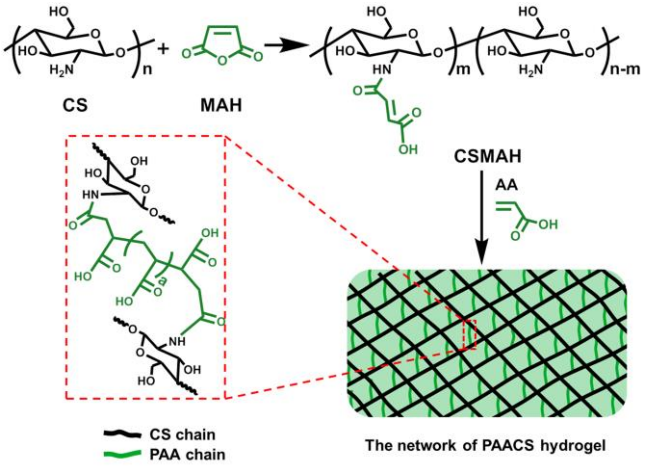

Scheme 2. Preparation of PAACS hydrogels.

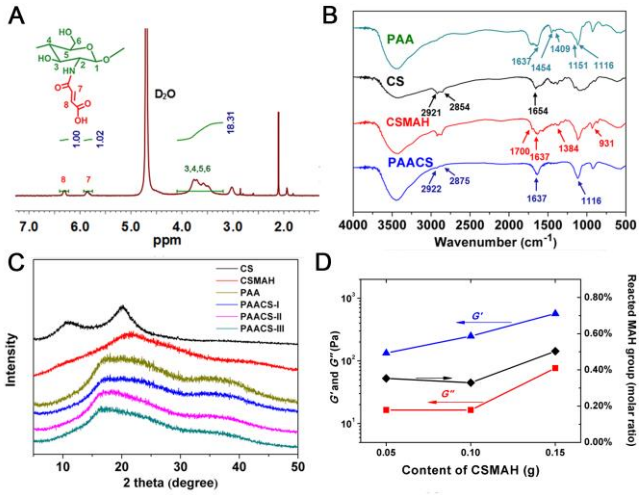

548

549 **Fig. 1.** ^{1}H NMR spectrum of CSMAH (A); FTIR spectra (B) and XRD patterns (C) of

550 CS, CSMAH, PAA and PAACS hydrogels; Elastic modulus *G'* and viscous modulus

551 *G''* of PAACS hydrogels as a function of frequency (D).

552

553

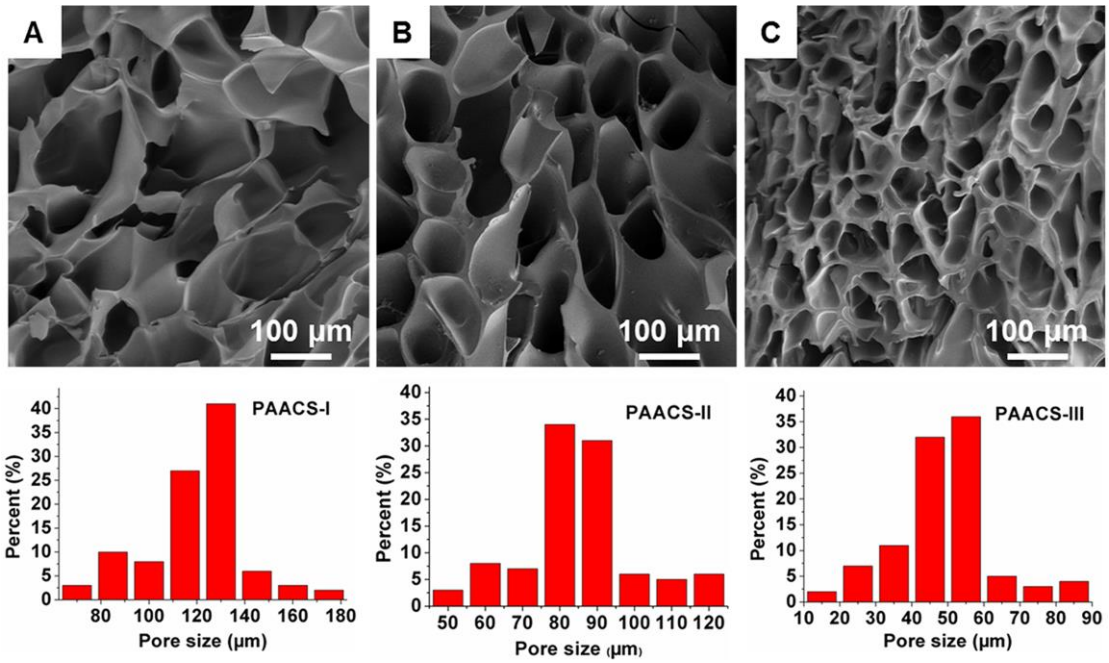

554

555 **Fig. 2.** The network structures and the pore size distributions of the hydrogels: A)

556 PAACS-I; B) PAACS-II; C) PAACS-III (each statistical result was obtained by

557 counting 100 pores from the SEM image).

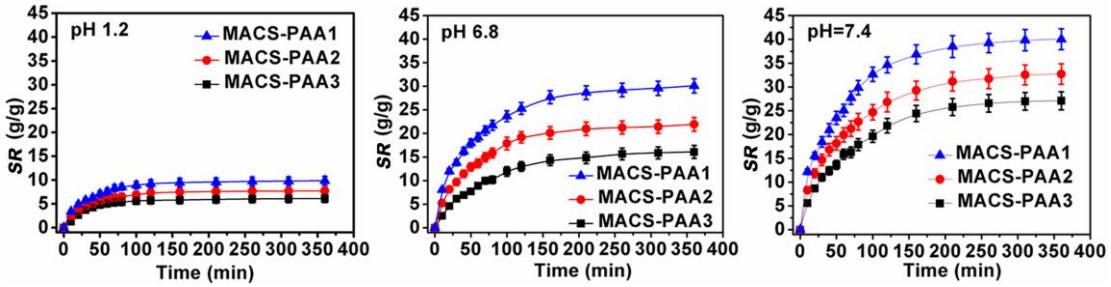

Fig. 3. Swelling kinetics of PAACS hydrogels at different pH, error bars are the standard error of the mean taken from three samples.

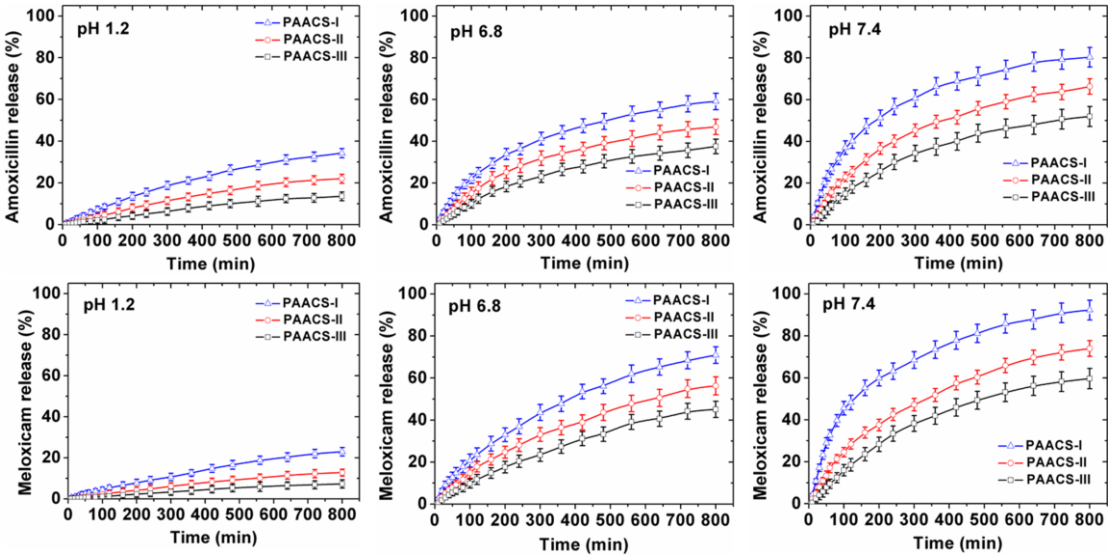

Fig. 4. The release curves of amoxicillin and meloxicam at different pH, error bars are the standard error of the mean taken from three samples.

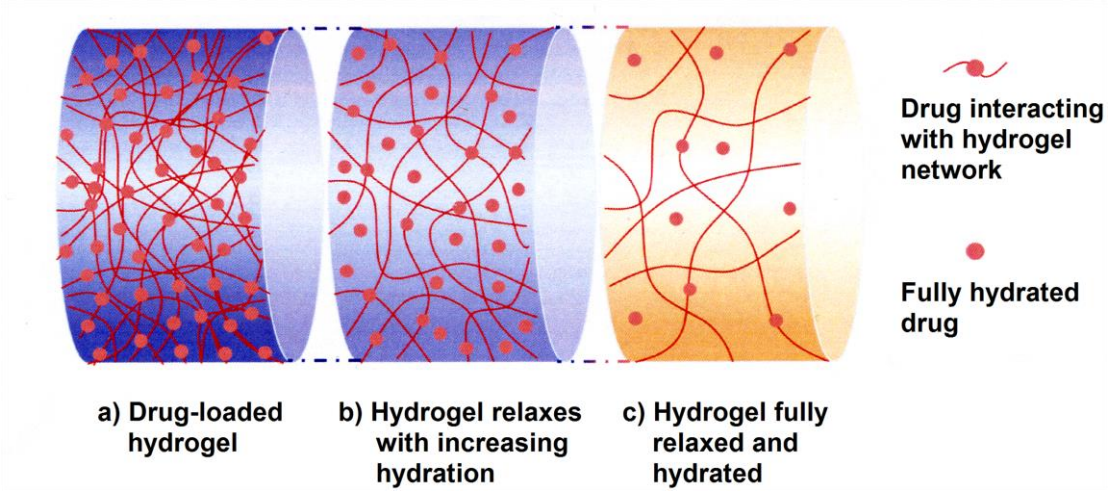

570

571 **Fig. 5.** Schemetic illustration of the process of drug release from hydrogel.